Appl Water Sci (2017) 7:115–127
DOI 10.1007/s13201-014-0223-5

ORIGINAL ARTICLE

Enhanced photocatalytic activity of metal oxides/β-cyclodextrin nanocomposites for decoloration of Rhodamine B dye under solar light irradiation

Subramanian Rajalakshmi · Sakthivel Pitchaimuthu · Nagarathinam Kannan · Ponnusamy Velusamy

Received: 10 May 2013 / Accepted: 11 July 2014 / Published online: 29 August 2014

Abstract We present the photocatalytic decoloration of Rhodamine B (RhB) dye with the nanocomposites such as TiO_2, ZnO, TiO_2/β-cyclodextrin (β-CD) and ZnO/β-CD. Band gap energy of nanocomposites was calculated by UV-DRS analysis and the results showed that the band gap energy of ZnO/β-CD nanocomposite is lower than that of other catalysts. The microstructures of the nanocomposites have been characterized by PXRD and FE-SEM analyses. The results showed that crystallinity and surface morphology of metal oxides (MO) (say, TiO_2 and ZnO) are not changed in MO/β-CD nanocomposite systems. GC–MS results showed that the photocatalytic decoloration of RhB follows the steps such as *N*-deethylation, cleavage of chromophore and mineralization of dye.

Keywords RhB · TiO_2 · ZnO · TiO_2/β-CD · ZnO/β-CD

Introduction

Rhodamine B (RhB) is a highly water soluble, basic red dye of xanthene class. It is found as a reddish violet powder and comes under the trade name of D and C red no. 19 (molecular formula = $C_{28}H_{31}ClN_2O_3$; molecular weight = 479.02). It is widely used as a colorant in textiles and food stuffs. It is also a well-known water tracer fluorescent. It causes irritation to skin, eyes and respiratory tract. The carcinogenicity, reproductive and developmental toxicity, neurotoxicity and chronic toxicity towards humans and animals have been experimentally proven (Jain et al. 2007; Kelesoglu et al. 2012; Dlamini et al. 2011).

The traditional ways of processing wastewater containing dyes through coagulation–flocculation or adsorption by activated carbon are inefficient since they just transfer the dye molecules from liquid to solid. In the past few years, photocatalysis using semiconductor has attracted more as a new and efficient method to treat wastewater containing colorants. It is well documented that TiO_2 and ZnO can only absorb a small fraction of sunlight (ultraviolet and near ultraviolet) due to their broad band gap (3.0–3.2 eV) and therefore, it is necessary to modify photocatalysts which can effectively be utilized the solar energy to a greater extent (Kou et al. 2012; Beltran-Heredia et al. 2011).

Cyclodextrins (CDs) are cyclic oligosaccharides composed of 6, 7 and 8 D-glucopyranose rings termed α-, β- and γ-CD, respectively. CDs are shaped like truncated cones, with a hydrophobic cavity and a hydrophilic exterior. The precise number of hydroxyl groups according to the number of glucose units makes it possible to establish strong interactions with other molecules and can form inclusion complexes with guest molecules (Serra-Gomez et al. 2012; Xin et al. 2012). As for the application of CD in environmental chemistry is concerned, it is more interesting and important to know if CD inclusion will change the environmental behavior and the fate of organic pollutants and if there could be any possibility to make use of CD in pollutants control (Zhang et al. 2007). Attarchi et al. prepared Ag/TiO_2/β-CD nanocomposite and tested its photocatalytic activity for degradation of methylene blue dye (Attarchi et al. 2013), Yang et al. (2014) reported the self-assembly of bioinspired catecholic cyclodextrin TiO_2

S. Rajalakshmi · S. Pitchaimuthu · N. Kannan · P. Velusamy (✉)
Centre for Research and Post-Graduate Studies in Chemistry, Ayya Nadar Janaki Ammal College, Sivakasi 626 124, Tamilnadu, India
e-mail: velusamyanjac@rediffmail.com

heterosupramolecule with high adsorption capacity and efficient visible-light photoactivity, photodegradation of 4,4-bis(4-hydroxyphenyl)valeric acid and its inclusion complex with β-cyclodextrin in aqueous solution (Salomatova et al. 2014) has been reported recently.

We have reported photocatalytic decoloration of dyes with TiO_2/β-CD and ZnO/β-CD using visible, UV and solar light and the results were compared with bare TiO_2 and ZnO (Velusamy et al. 2011, 2013; Rajalakshmi et al. 2013; Pitchaimuthu et al. 2013; Velusamy et al. 2014). The present study is aimed to investigate the feasibility of solar light for photocatalytic decoloration of RhB dye in different conditions. The effect of various parameters such as initial dye concentration, irradiation time, amount of catalysts and pH have been investigated on the photocatalytic decoloration of RhB in the presence of TiO_2/β-CD and ZnO/β-CD as a photocatalyst and the results were compared with bare TiO_2 and ZnO. The mineralization of RhB dye was further confirmed by Chemical Oxygen Demand (COD). A decoloration pathway based on GC–MS was studied to confirm the photocatalytic decoloration of RhB dye.

Experimental

Materials

RhB dye obtained from Loba Chemie (India) was used as such. The catalysts viz, TiO_2 and ZnO were received from SD fine chemicals, India. β-CD was purchased from Hi Media Chemicals (P) Ltd. All the other chemicals and reagents were used as received.

Samples preparation

Reported procedures were employed for the preparation of RhB/β-CD complex (Pitchumani et al. 1994; Velusamy et al. 2011, 2014). To a saturated solution of β-CD in distilled water, equimolar amount of RhB dye was added and stirred continuously for 24 h. The precipitated inclusion complex was filtered and washed with diethyl ether to remove uncomplexed RhB dye and dried in an air oven at 60 °C for 2–3 h. The precipitate thus obtained is used for the characterization of RhB/β-CD complex by FT-IR and ^{1}H NMR analyses.

Metal oxides (MOs) such as TiO_2 and ZnO were added into 0.01 mol/L β-CD solution and stirred for 20 min. The suspended solution was centrifuged; the solids were separated and washed three times with water. The solids were dried with an infrared lamp for UV-DRS, PXRD and FE-SEM analyses (Lu et al. 2004).

Exactly 10×10^{-6} M of RhB dye was prepared using deionised water and various concentrations of β-CD like 1.25, 2.50, 3.75, 5.00, 6.25 and 7.50×10^{-5} M were prepared in a 25 mL SMF. These two solutions were mixed thoroughly with magnetic stirrer for 24 h. Then these samples were analyzed with UV–visible spectrophotometer (Velusamy 1998).

For GC–MS analysis, the photocatalytic decoloration experiments were carried out under different irradiation times and irradiated samples were collected. The dye solution was extracted using $CHCl_3$ as a solvent. The solvent was evaporated. The residue was then used for the analyses.

Characterization

X-ray diffraction patterns of powder samples were recorded with a high-resolution powder X-ray diffractometer model RICH SIERT & Co with CuK_α radiation as the X-ray source ($\lambda = 1.5406 \times 10^{-10}$ m). FE-SEM images were obtained on a Carl ZEISS (ΣIGMA Series, Germany) microscope taken at an accelerated voltage of 2 kV. UV–visible diffuse reflectance spectra were recorded on a Shimadzu 2550 UV–visible spectrophotometer with $BaSO_4$ as the background between 200 and 700 nm. NMR spectra were recorded at 400 MHz Bruker NMR spectrometer (in DMSO–d_6). UV–visible spectra were recorded using UV–visible spectrophotometer (Shimadzu UV-1700) and the scan range was from 400 to 800 nm. FT-IR spectra were recorded using FT-IR spectrometer (Shimadzu model 8400S) in the region 4,000–400 cm^{-1} using KBr pellets. Absorbance of the dye was determined with visible spectrophotometer (ELICO-207). The pH of the dye solution was measured using digital pen pH meter (HANNA instrument, Portugal). The GC–MS spectra was recorded by GC (Perkin-Elmer Auto System) equipped with an HP5-MS capillary column (30 × 250 micron) and 1-μm film thickness (Perkin-Elmer elite series) and interfaced directly to the MS (Perkin-Elmer turbo mass spectrophotometer). The GC column was operated at a temperature of 50 °C for 2 min then increased to 280 °C at the rate of 10 °C/min in split mode. Injection volume 0.1 μL with helium as carrier gas was used. The other analytical conditions are: EI impact ionization 70 eV, injection temperature 280 °C, source temperature 180 °C.

Photocatalytic experiments

All experiments were carried out under identical conditions using Borosilicate beakers as the sample holders. Exactly 50 mL of RhB dye solution with required amount of

catalysts and at definite concentration was irradiated under solar light. Prior to irradiation, the reaction mixture was stirred in the dark for 20 min to achieve adsorption saturation. At regular intervals, 5 mL of the sample was taken out and centrifuged to remove the catalysts. Absorbance at 544 nm was measured to determine the concentration of RhB after the photocatalytic decoloration process. The photocatalytic reaction was carried out during the daytime. The light intensity during the photocatalytic reaction was measured using lux meter (between 11.30 AM to 1.30 PM) and found that it was in the range of 944–1,090 lux. COD analyses were done by open reflux method (Alhakimi et al. 2003).

Results and discussion

Characterization of photocatalysts

Optical properties

UV–visible diffuse reflectance spectra of TiO_2, ZnO, TiO_2/β-CD and ZnO/β-CD give information about the optical properties of the catalysts. The reflectance data reported as $(\alpha hv)^2(eV)^2$ values have been obtained by the application of the Kubelka–Munk algorithm. The band gaps of the catalysts have been deduced from the Tauc plot. Figure 1 indicates the plot of $(\alpha hv)^2(eV)^2$ vs energy. The extrapolation of the rising segment of $(\alpha hv)^2(eV)^2$ to the abscissa at zero F® provides the band gap energy as 3.35 eV for TiO_2, 3.27 eV for ZnO, 3.31 eV for TiO_2/β-CD and 3.23 eV for ZnO/β-CD nanocomposites. The results showed that the band gap energy of MO/β-CD nanocomposites is lower

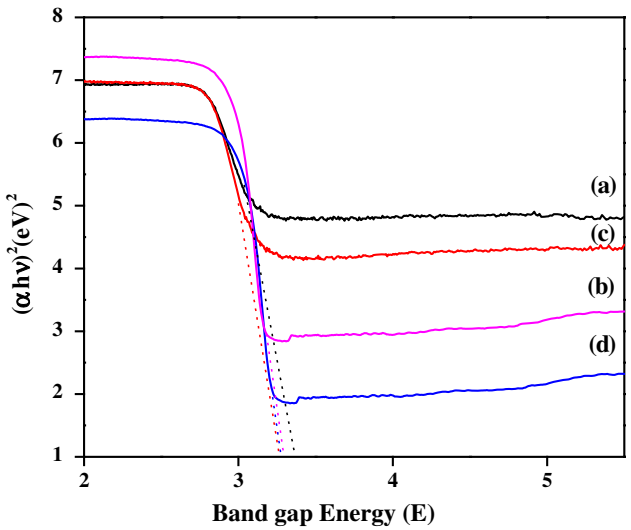

Fig. 1 Diffuse reflectance spectra of *a* TiO_2, *b* ZnO, *c* TiO_2/β-CD, *d* ZnO/β-CD

than the corresponding metal oxides. Therefore, MO/β-CD nanocomposites can be excited to produce more electron–hole pairs under same light illumination which could result in higher photocatalytic activity (Karunakaran et al. 2010).

Phase structure

The XRD patterns of TiO_2/β-CD and ZnO/β-CD nanocomposites are similar to that of TiO_2 and ZnO particles (Rajalakshmi et al. 2013). The XRD analysis of TiO_2 reveals that the sample exhibits single phase belongs to anatase-type TiO_2 which is identified by comparing the spectra with the JCPDS file # 21-1272 (Velusamy et al. 2014; Pitchaimuthu et al. 2013). Diffraction peaks at 25.38°, 37.90°, 48.07°, 53.94° and 55.18° correspond to (101), (004), (200), (105) and (211) planes of TiO_2, respectively. The XRD spectra of ZnO and ZnO/β-CD composites provide all of the characteristic peaks which are well matched with that of hexagonal wurtzite ZnO (JCPDS file # 36-1451) (Velmurugan and Swaminathan 2011). The relatively high intensity of the peak for (101) plane is an indicative of anisotropic growth and implies a preferred orientation of the crystallites. The peaks corresponding to the MOs exhibit appreciable differences in MO/β-CD nanocomposites. In particular, the peaks related to β-CD of 2θ values from 12.38° to 12.70° are hidden and the peaks of 2θ values are getting reduced when it is blended with TiO_2. In the same way, the peaks correspond to ZnO of 2θ values at 31.74°, 31.76°, 31.78° and 36.18° to 36.36° are getting reduced when ZnO is blended with β-CD. All the above evidences imply that there is a strong binding between β-CD and MOs. This indicates that the incorporation of β-CD on MOs provide no change in the crystalline structure of the bare TiO_2 and ZnO. But the main peak intensity of the both TiO_2/β-CD and ZnO/β-CD nanocomposites are slightly lower than bare TiO_2 and ZnO.

Morphology

The morphology of the samples was investigated by FE-SEM analyses. Figure 2a–e depicts FE-SEM of β-CD, TiO_2, ZnO, TiO_2/β-CD and ZnO/β-CD nanocomposites, respectively. The surface morphology of pristine β-CD (Fig. 2a) shows its amorphous nature. TiO_2 crystals have spherical morphology with uniform particle size (Fig. 2b). ZnO has prismatic morphology with uniform particles containing wurtzite lattice structure (Fig. 2c). Whereas in TiO_2/β-CD nanocomposites (Fig. 2d) and ZnO/β-CD (Fig. 2e), two different types of particles are observed. The smaller size particles correspond to β-CD and larger particles correspond to MOs such as TiO_2 and ZnO. This indicates that the β-CD molecules are

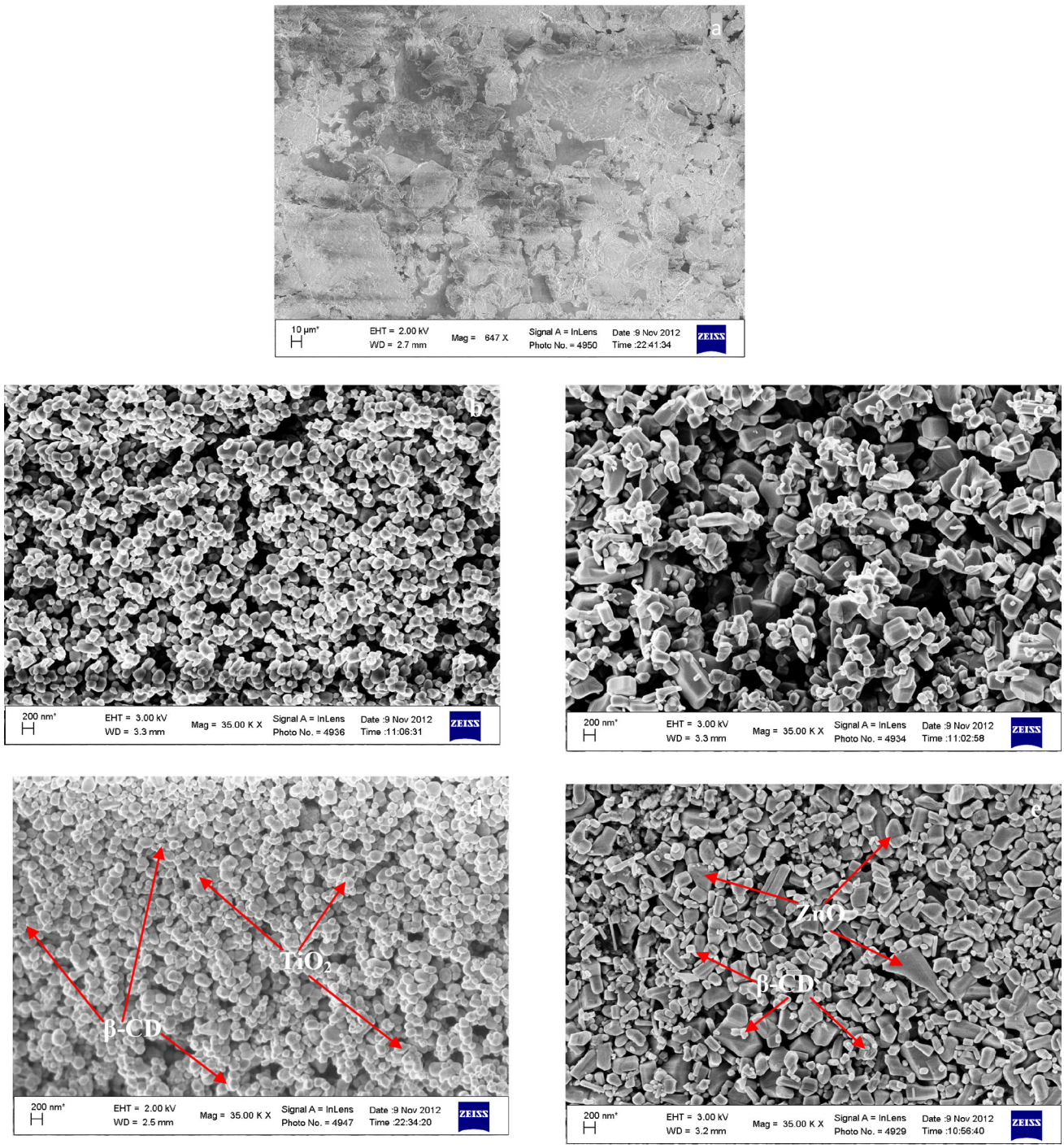

Fig. 2 FE-SEM images of **a** β-CD, **b** TiO_2, **c** ZnO, **d** TiO_2/β-CD, **e** ZnO/β-CD

adsorbed on the surface of the metal oxides. It is also observed that the surface of MO nanocomposites (TiO_2/β-CD and ZnO/β-CD) is very loosely backed in nature. This kind of surface can provide a better adsorption environment and more active sites for the photocatalytic decoloration reactions.

Evidence for complex formation

Dissociation constant measurement

Based on UV-absorption spectral studies (using the Benesi and Hildebrand equation) (Pitchumani et al. 1994;

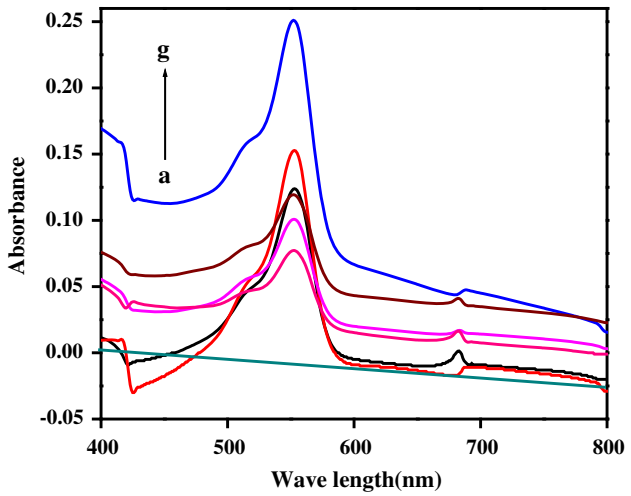

Fig. 3 UV-visible spectra for complexation of RhB/β-CD *a* β-CD, *b* RhB, *c* 1:1 RhB/β-CD, *d* 1:2 RhB/β-CD, *e* 1:3 RhB/β-CD, *f* 1:4 RhB/β-CD, *g* 1:5 RhB/β-CD

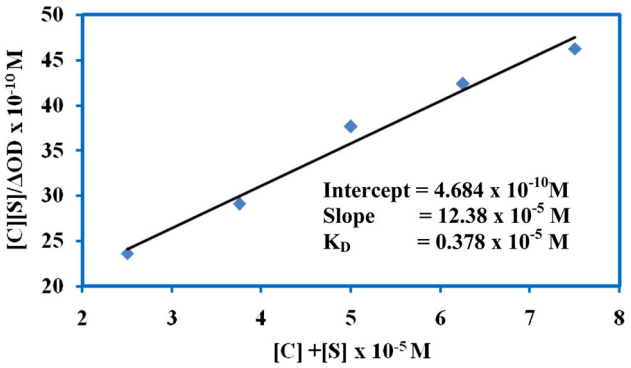

Fig. 4 Plot of [C] [S]/Δ OD vs {[C] + [S]} for RhB/β-CD complex

Velusamy 1998), the dissociation constant (K_D) is evaluated as 0.378×10^{-5} M (Figs. 3, 4). The value of K_D indicated that the dye molecules form strong inclusion complex with β-CD.

FT-IR spectra

FT-IR techniques are not generally utilized for the detection of inclusion compounds because the resultant spectra have super position of host and guest bands. However, in this study RhB dye has some characteristics FT-IR absorption in regions where β-CD does not show absorption in the corresponding regions is used to identify the host–guest interaction (Velusamy et al. 1996). FT-IR spectra of complexation between RhB dye and β-CD (1:1) and its physical mixture (1:1) are presented in Fig. 5. The aromatic –C–H stretching of RhB is observed at 2,977.89 cm^{-1} is shifted with reduced intensity to 2,972.74 cm^{-1} in the RhB/β-CD complex. Similarly, the peaks at the frequencies 1,640.17, 1,577.66, 1,640 and

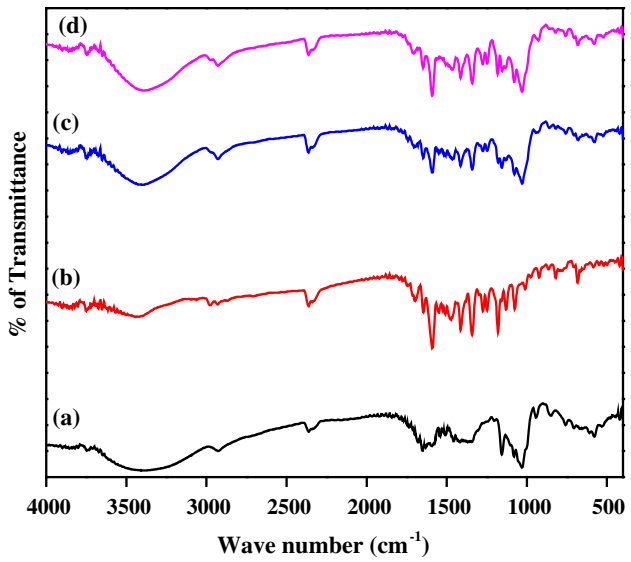

Fig. 5 FT-IR spectra of *a* β-CD, *b* RhB, *c* 1:1 physical mixture of RhB/β-CD, *d* 1:1 complex of RhB/β-CD (KBr pellets)

894.91 cm^{-1} corresponding to the functional groups such as –COOH, –C=C–, –C–N= and –C–O–C– are shifted to 1,706.88, 1,589.23, 1,647.10 and 1,182.28 cm^{-1}, respectively, in the RhB/β-CD complex. It indicates that there is a strong inclusion complex between RhB and β-CD.

^1H NMR analysis

Formation of an inclusion complex between RhB and β-CD was also inferred from ^1H NMR studies of RhB/β-CD complex. The chemical shifts (in ppm) given for β-CD protons are shifted in RhB/β-CD complex (Fig. 6; Table 1). The upfield shift was occurred for H_1 and H_3 and H_5, which are located in the inner side of β-CD. The changes of chemical shift ($\Delta\delta$) of H_3 and H_5 suggested that the RhB dye molecules are encapsulated into the hydrophobic cavity of β-CD. On the contrary, the chemical shifts of H_2 and H_4 which are located on the outer surface of β-CD and the narrow opening of β-CD, undergo downfield shift by the RhB dye molecules. H_6 proton does not undergo any changes. Similarly, for RhB protons there is no change in H_c protons and H_a and H_b protons are shifted to upfield because of the interaction between RhB and β-CD (Table 2). These observations are consistent with the notation that the phenyl ring of RhB dye molecule is suitably encapsulated into the β-CD cavity.

Assessment of photocatalytic activity

Effect of initial concentration

The photocatalytic decoloration of RhB dye was carried out by varying the initial concentration of the dye and

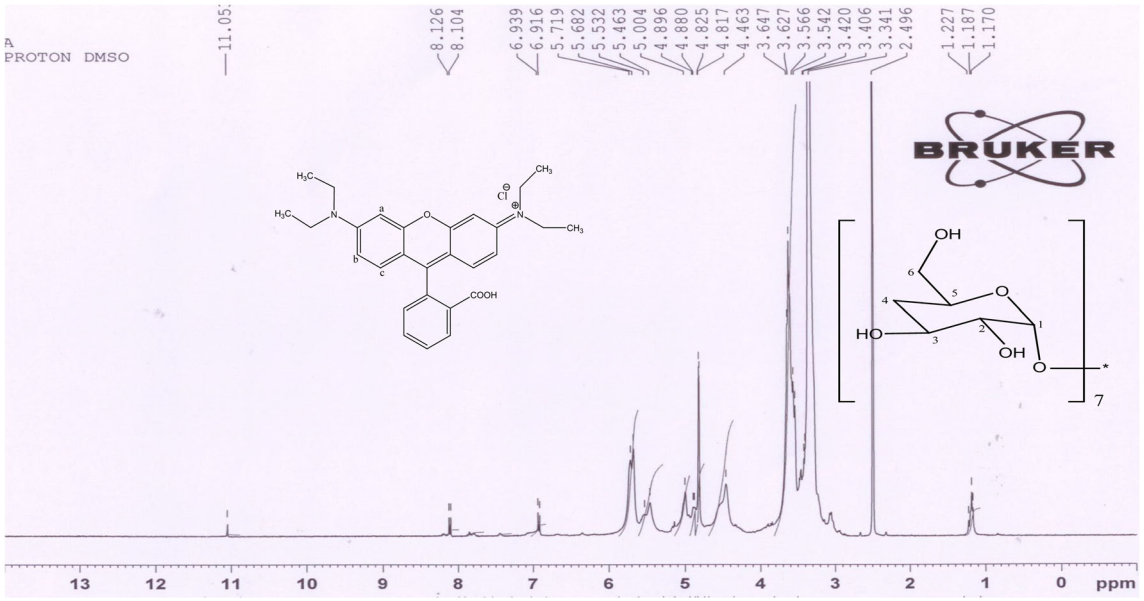

Fig. 6 ^{1}H NMR spectra of RhB/β-CD inclusion complex (DMSO-d_6)

Table 1 ^{1}H NMR chemical shifts of β-CD protons in RhB/β-CD complex

	H_1	H_2	H_3	H_4	H_5	H_6
β-CD	5.03	4.00	3.73	3.02	3.73	3.54
RhB/β-CD	5.00	4.46	3.65	3.34	3.65	3.54
$\Delta\delta$	0.03	−0.46	0.08	−0.32	0.08	0.00

Chemical shifts values are expressed in ppm

Table 2 ^{1}H NMR chemical shifts of RhB protons in RhB/β-CD complex

	H_a	H_b	H_c
RhB	5.85	5.94	6.91
RhB/β-CD	5.53	5.72	6.91
$\Delta\delta$	0.32	0.22	0.00

Chemical shifts values are expressed in ppm

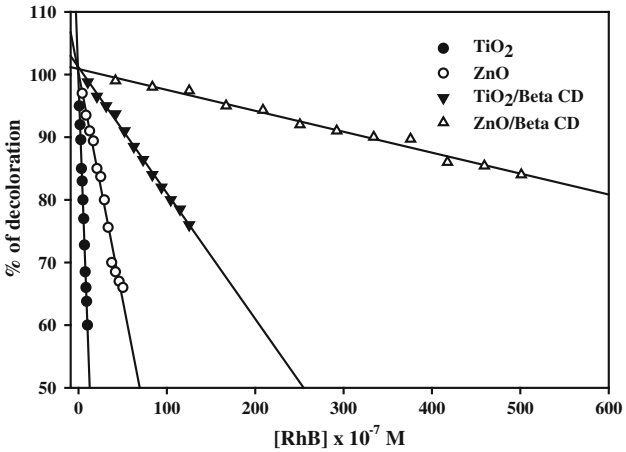

Fig. 7 Effect of initial concentration on photocatalytic decoloration of RhB dye under solar light irradiation time = 120 min; dose = 2 g/L; pH = 3.6

fixing all other processing parameters constant. Figure 7 shows that the percentage of decoloration decreases with increase in initial concentration of RhB from 95.0 to 60.0 % for TiO_2, 97.0–66.0 % for ZnO, 98.8–76.0 % for TiO_2/β-CD and 99.0–84.0 % for ZnO/β-CD nanocomposite. The possible explanation for this behavior is that as the initial concentration of the dye increases (1) the path length of the photons entering into the solution decreases and in low concentration the reverse effect is observed, thereby increasing the number of photon absorption by the catalyst in lower concentration and hence percentage of decoloration decreases. (2) Due to the lack of active sites with the increase in the initial concentration of RhB, the amount of dye adsorbed on the catalyst surface gets increased. Due to this, only fewer photons reach at the surface of photocatalyst. This results decrease in concentration of $^{\bullet}OH$ and $O_2^{\bullet-}$ radicals thereby decrease in photocatalytic decoloration activity (Wang et al. 2008; Aliabadi and Sagharigar 2011; Dong et al. 2010). From the results it was also inferred that the 167×10^{-7} M concentration of RhB dye was decolorized up to 95.0 % using ZnO/β-CD nanocomposite at the optimum reaction conditions such as irradiation time = 120 min; dose = 2 g/L and pH = 3.6.

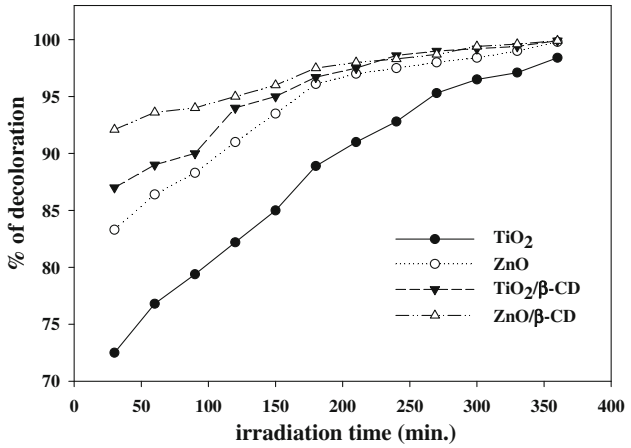

Fig. 8 Effect of irradiation time on photocatalytic decoloration of RhB dye under solar light irradiation. [RhB] = 4.1×10^{-7} M for TiO_2, 16.7×10^{-7} M for ZnO, 41.7×10^{-7} M for TiO_2/β-CD, 167×10^{-7} M for ZnO/β-CD; dose = 2 g/L; pH = 3.6

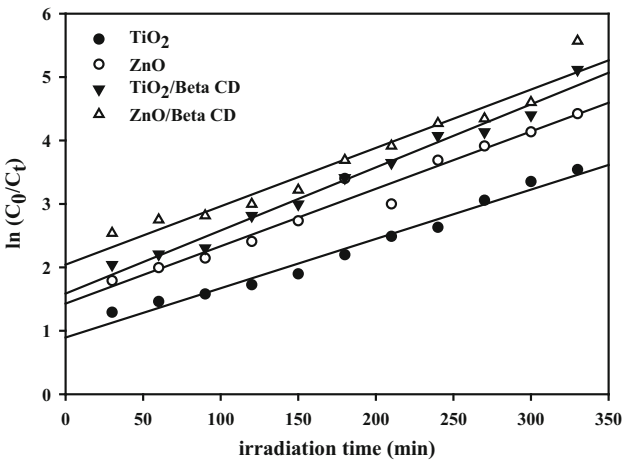

Fig. 9 Kinetics of photocatalytic decoloration of RhB dye under solar light irradiation

Effect of irradiation time

The effect of irradiation time for the removal of RhB dye by semiconductor mediated photocatalysis is shown in Fig. 8. It has been found that with the increase in irradiation time, percentage of decoloration increases from 72.5 to 98.4 % for TiO_2, 83.3–99.8 % for ZnO, 87.0–99.9 % for TiO_2/β-CD and 92.1–99.9 % for ZnO/β-CD nanocomposite. This is attributed to the fact that, as the irradiation time is increased, the dye molecules have enough time to react with the catalysts and form hydroxyl radicals which accelerate photocatalytic decoloration reaction and also as time proceeds, this concentration gradient decreases due to accumulation of dye molecules on vacant sites and thus saturation stage was almost perceived and hence percentage of decoloration increases (Daneshvar et al. 2003a, b).

Kinetics of photocatalytic decoloration

Reaction kinetics gives enough information about the reaction rates and the mechanisms by which the reactants are converted to the products. Kinetics is determined for all the catalysts as ln C_0/C_t vs irradiation time after the photocatalytic decoloration process (Fig. 9). The results showed that the photocatalytic decoloration of RhB obeys apparently pseudo-first-order kinetics and the rate expression is given by

$$\ln C_0/C_t = kt \quad (1)$$

where C_t is the concentration of RhB at time t, C_0 is the initial concentration of RhB and k is the pseudo-first-order rate constant (Wang et al. 2009a, b).

Effect of amount of catalysts

Effect of amount of catalysts is an important factor that affects the photocatalytic decoloration reactions. Experiments were performed by varying the amount of catalysts from 0.6 to 7.2 g/L. The results (Fig. 10) showed that the percentage of photocatalytic decoloration increased by increasing the amount of catalysts from 76.5 to 89.5 % for TiO_2, 85.0–96.8 % for ZnO, 88.0–98.8 % for TiO_2/β-CD and 90.5–99.5 % for ZnO/β-CD nanocomposite. Irrespective of the nature of the dye and photocatalysts, the percentage of removal was found to enhance linearly (certain level) with increase in the dose of the catalyst indicating the heterogeneous regime. This may probably be due to: (1) increase in the extent of dye adsorption molecules on the catalyst surface; (2) increase in the number of surface active sites; (3) enhanced generation of hydroxyl radicals due to increase in the concentration of charge carriers. However, at higher amount of catalyst, the reaction rate tends to decrease which may be attributed to; (1) the deactivation of activated molecules by collision with ground state molecules; (2) the agglomeration of the catalyst particles at higher amount of catalysts, which covers the part of photosensitive area retarding the photon absorption and also the dye adsorption; (3) turbidity at higher amount of catalysts results in the shadowing effect thus decreasing the penetration depth of light irradiation; (4) high degree of scattering by the catalyst particles and increase in the opacity. Hence above a certain level, the additional catalyst amount does not get involved in catalytic activity and further increment in the reaction rate was not observed. Hence, the optimum level of dose is 2 g/L (Daneshvar et al. 2003a, b; Grzechulska and Morawski 2002; Wang et al. 2009a, b; Rauf and Salman Ashraf 2009; Damardji et al. 2009; Chen et al. 2004).

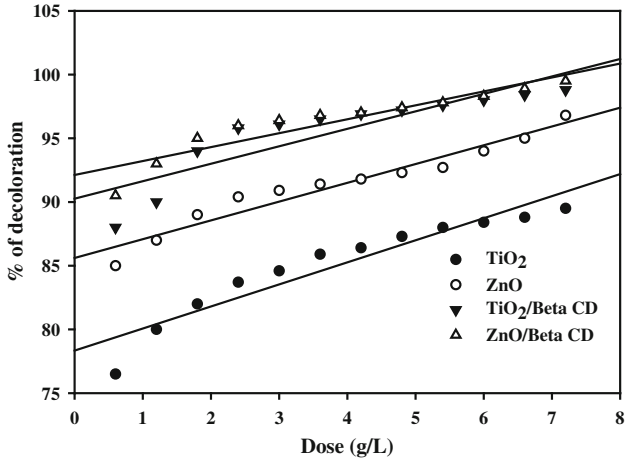

Fig. 10 Effect of amount of catalysts on photocatalytic decoloration of RhB dye under solar light irradiation. [RhB] = 4.1×10^{-7} M for TiO_2, 16.7×10^{-7} M for ZnO, 41.7×10^{-7} M for TiO_2/β-CD, 167×10^{-7} M for ZnO/β-CD; irradiation time = 120 min; pH = 3.6

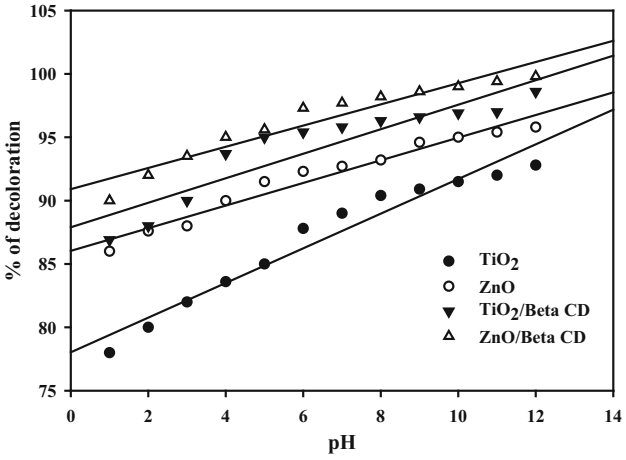

Fig. 11 Effect of pH on photocatalytic decoloration of RhB dye under solar light irradiation. [RhB] = 4.1×10^{-7} M for TiO_2, 16.7×10^{-7} M for ZnO, 41.7×10^{-7} M for TiO_2/β-CD, 167×10^{-7} M for ZnO/β-CD; irradiation time = 120 min; dose = 2 g/L

Effect of pH

The pH of the aqueous solution is an important variable in the evaluation of aqueous phase-mediated photocatalytic reactions. The effect of pH on the photocatalytic decoloration of RhB dye was studied under constant experimental conditions such as amount of catalysts (2 g/L), irradiation time (120 min) and concentration of the dye [4.1×10^{-7} M (TiO_2); 16.7×10^{-7} M (ZnO); 41.7×10^{-7} M (TiO_2/β-CD); 167×10^{-7} M (ZnO/β-CD)]. The experiments were carried out by changing in the initial pH value of the dye from 1 to 12. It has been observed from Fig. 11 that the percentage of decoloration increased considerably with an increase in pH from 78.0 to 92.8 % for TiO_2, 86.0–95.8 % for ZnO, 86.9–98.6 % for TiO_2/β-CD and 90.0–99.8 % for ZnO/β-CD nanocomposite and it showed percentage of decoloration is higher at strong basic condition than the neutral pH. The reason is under alkaline conditions, the concentrations of perhydroxyl radicals and hydroxide ions are getting increased. During catalyst-based photochemical reactions, both perhydroxyl as well as hydroxyl ions produce large number of hydroxyl radicals in the aqueous medium, which effectively take part in the decoloration of organic pollutants present in RhB dye (Wang et al. 2009a, b; Kansal et al. 2008; Santhi et al. 2011).

$$\mathrm{pH} > \mathrm{pH_{ZPC}} \quad \mathrm{M-OH} + \mathrm{OH^-} \rightarrow \mathrm{MO^-} + \mathrm{H_2O} \qquad (2)$$

$$\mathrm{pH} < \mathrm{pH_{ZPC}} \quad \mathrm{M-OH} + \mathrm{H^+} \rightarrow \mathrm{MOH_2^+} \qquad (3)$$

The pH of the reaction has a significant effect on the surface properties of the metal oxide photocatalysts, which include the surface charge of the particles, the extent of aggregation of the catalyst particles, and the band edge position of metal oxides. The zero charge point (pH_{ZPC}) for ZnO is 8.8 and TiO_2 is at 6.2. The extent of positive charges on the metal oxide surface decreases with increasing pH and reaches zero at pH_{ZPC}. Therefore, pH significantly affects the adsorption–desorption properties of the compounds on the surface of the catalysts. At $pH > pH_{ZPC}$, MO^- is the predominant species, whereas at $pH < pH_{ZPC}$, MOH_2^+ is the predominant species according to the Eqs. (2) and (3).

Determination of COD

As the reduction of COD reflects the extent of photocatalytic decoloration of an organic species, the reduction of COD was studied as a function of pH using solar light irradiation.

Figure 12 presents the comparison between removal of COD of RhB with all the catalysts and shown that the COD decreases with increase in pH and initial COD values (460.6 mg O_2/L for TiO_2; 458.4 mg O_2/L for ZnO; 401.06 mg O_2/L for TiO_2/β-CD and 346.07 mg O_2/L for ZnO/β-CD) were reduced after photocatalytic decoloration process. COD is significantly reduced with ZnO/β-CD nanocomposites up to 18.09 % than other catalysts (Dukkanci et al. 2010).

Role of β-CD for the enhancement of photocatalytic activity of catalysts

A suitable mechanism for the photocatalytic decoloration of RhB with MO/β-CD is proposed as given below (Eqs. 4–12) and also schematically represented

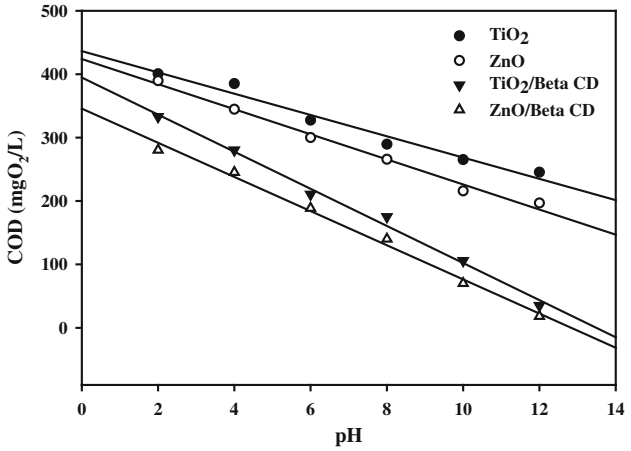

Fig. 12 Determination of COD for photocatalytic decoloration of RhB dye under solar light irradiation. [RhB] = 4.1×10^{-7} M for TiO_2, 16.7×10^{-7} M for ZnO, 41.7×10^{-7} M for TiO_2/β-CD, 167×10^{-7} M for ZnO/β-CD; irradiation time = 120 min; dose = 2 g/L

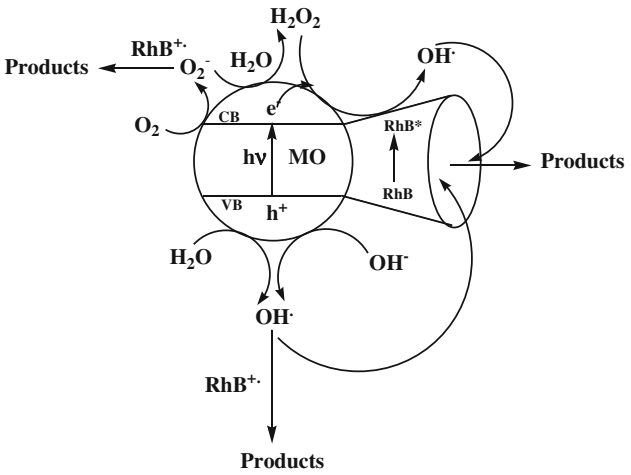

Scheme 1 Mechanism for the enhancement of photocatalytic decoloration of RhB dye with MO/β-CD systems

in Scheme 1. The RhB dye enters into the cavity of β-CD, which is linked to the MO surface in the equilibrium stage. Since CDs have higher affinity for the MO surface than RhB, β-CD molecules could adsorb on the surface of the MO and occupy the reaction sites β-CD would capture holes on the active surface of MO resulting in the formation of stable MO/β-CD complex (Eq. 4). Hence, the reaction between the reactants such as RhB and MO/β-CD complex should be the key step in the photocatalytic degradation of RhB in MO suspension containing β-CD (Eq. 5) (Zhang et al. 2011). An electron is rapidly injected from the excited RhB to the conduction band (Hoffmann et al. 1995; Macwan et al. 2011; Zhang et al. 2009; Wang et al. 2006a). The enhancement of photocatalytic decoloration of RhB mainly resulted in the enhanced adsorption of RhB on MO surface and moderate inclusion depth of RhB in the β-CD cavity. Since β-CD can include the RhB into its cavity and adsorbed onto the surface of MO, it could play a role as bridge or channel for RhB to get onto the MO surface and accumulate the higher concentrations, which makes the decoloration of RhB more easy and effective in the presence of hydroxyl radicals produced during photocatalytic decoloration processes. MO/β-CD system apparently exhibited declined photoluminescence intensity compared with MO system which indicates that the electron/hole recombination has been suppressed in the MO/β-CD nanocomposite systems. Therefore, the quantum efficiency of MO has been enhanced as the recombination of e^-_{CB}/h^+_{VB} is getting lowered, which resulted in the generation of more hydroxyl and superoxide radicals (Eqs. 6–9). Thus, the decoloration of the RhB and $RhB^{+\bullet}$ could be accelerated which leads to the formation of mineralized products (Eqs. 10–12) (Wang et al. 2006b; Lu et al. 2004).

Fig. 13 GC-MS spectra for the photocatalytic decoloration of RhB dye under solar light irradiation

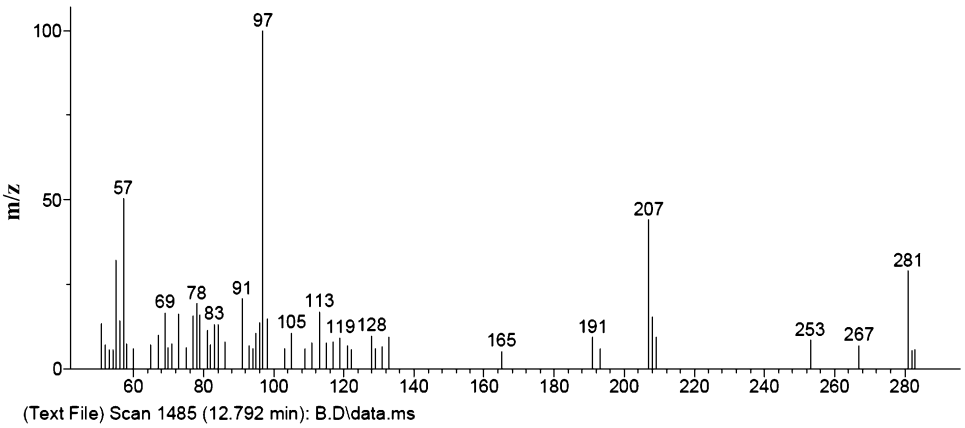

Scheme 2 Photocatalytic decoloration pathway for the photocatalytic decoloration of RhB dye under solar light irradiation

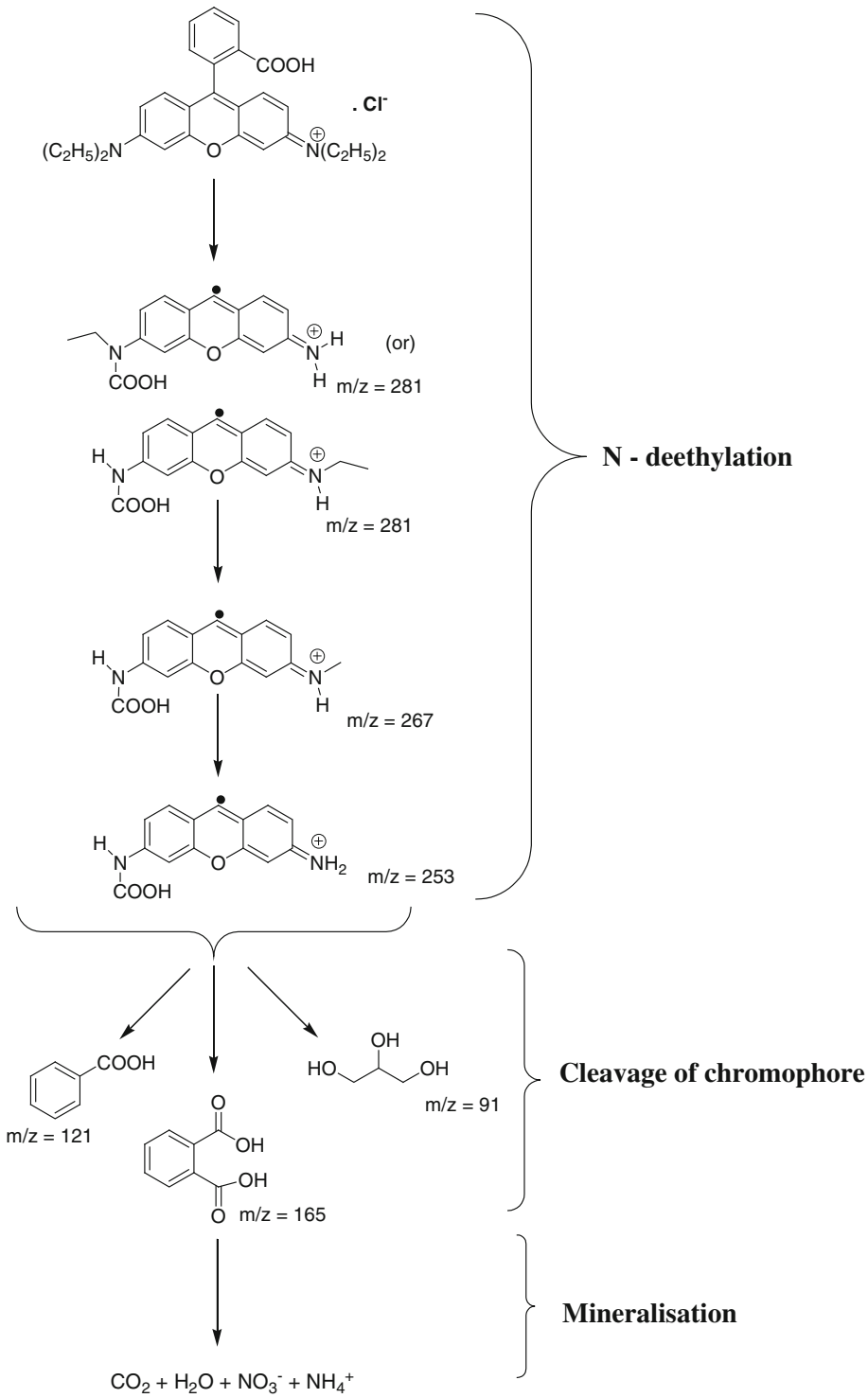

$$MO + \beta - CD \rightarrow MO/\beta - CD \quad (4)$$

$$RhB + MO/\beta - CD \rightarrow MO/\beta - CD^{\bullet}RhB \quad (5)$$

$$MO/\beta - CD^{\bullet}RhB + h\nu \rightarrow MO/\beta - CD^{\bullet 1}RhB* + MO/\beta - CD^{\bullet 3}RhB* \quad (6)$$

$$MO/\beta - CD^{\bullet 3}RhB* \rightarrow (e)MO/\beta - CD + RhB^{\bullet +} \quad (7)$$

$$MO/\beta - CD^{\bullet 1}RhB* + O_2 \rightarrow MO/\beta - CD^{\bullet}RhB + {}^1O_2 \quad (8)$$

$$(e)MO/\beta - CD + O_2 \rightarrow MO/\beta - CD + O_2^- \quad (9)$$

$$RhB^{+\bullet} \rightarrow \text{Products} \quad (10)$$

$$RhB + {}^{1}O_2 \rightarrow \text{Products} \quad (11)$$

$$RhB + {}^{\bullet}O_2^{-} \rightarrow \text{Products} \quad (12)$$

Photocatalytic pathway for the photodecoloration of RhB dye

Identification of possible intermediate products during the photocatalytic reaction is the best way to understand the photocatalytic decoloration reaction mechanism. To study the photocatalytic decoloration pathway of RhB dye under solar light irradiation as well as to identify the possible intermediate products during the photocatalytic decoloration, experiments were conducted with ZnO/β-CD as a photocatalyst. GC–MS spectra of the irradiated aqueous solutions of RhB at different time intervals were observed with the time interval of 60 min. Major intermediates during the photocatalytic decoloration process were proposed using m/z ($M - 1$) values of the GC–MS spectra (Fig. 13). Normally, RhB dye was found to be very stable under solar light irradiation in the absence of catalysts. Based on the results of GC–MS spectra, the fragmentation pathway and intermediates for the solar light-induced photocatalytic decoloration of RhB dye have been proposed and shown in Scheme 2. In photocatalytic decoloration of RhB dye three main steps are involved. They are (1) *N*-deethylation, (2) cleavage of chromophore, (3) mineralization of dye. N-deethylation followed by carboxylation lead to the formation of possible isomerized intermediates corresponding to the m/z value of 281. After carboxylation, the formed intermediate degraded into possible intermediate with m/z values of 267 and 253 and m/z values 121, 165 and 91 indicates that the RhB dye molecule is effectively oxidized by the catalysts into smaller molecules such as benzoic acid, phthalic acid and propane 1,2,3-triol. The formed oxidized products were then mineralized into CO_2, H_2O, NO_3^- and NH_4^+ as reported in literatures (Kansal et al. 2007; Yu et al. 2009; Sun et al. 2009; He et al. 2009; Luan et al. 2011; Silva et al. 2011; Mehrdad et al. 2011; Li et al. 2007).

Conclusions

In summary, ZnO/β-CD nanocomposite shows superior photocatalytic activities towards photocatalytic decoloration of RhB dye under solar light irradiation, which is due to the lower band gap energy of ZnO in ZnO/β-CD system. Moreover, concentration of RhB, irradiation time, dose of the catalysts used and pH of the reaction medium have significant effects on photocatalytic decoloration of RhB dye. β-CD can include the RhB into its cavity and is adsorbed onto the surface of MO, it could play a role as bridge or channel for RhB to get onto the MO surface and accumulate the higher concentrations, which makes the decoloration of RhB more easily and effectively in the presence of hydroxyl radicals produced during photocatalytic decoloration processes. The GC–MS spectral studies confirm the photocatalytic decoloration pathway of RhB dye which follows the steps such as *N*-deethylation, cleavage of chromophore and mineralization of dye. Based on the findings, ZnO/β-CD nanocomposite can be used as an efficient photocatalyst for the photocatalytic decoloration of RhB dye.

Acknowledgments The authors thank the Management and the Principal of Ayya Nadar Janaki Ammal College, Sivakasi, India for providing necessary facilities. The University Grants Commission, New Delhi, is greatly acknowledged for providing financial support through UGC-Major Research Project [UGC—Ref. No. F. No. 38-22/2009 (SR) Dated: 19.12.2009]. Authors also acknowledged Bharadithasan University, Trichy for recording FE-SEM, ^{1}H NMR spectra and GC–MS analyses and Department of Earth Science, Pondicherry University, Pondicherry for recording PXRD spectrum.

References

Alhakimi G, Studnicki LH, Al-Ghazali M (2003) Photocatalytic destruction of potassium hydrogen phthalate using TiO_2 and sunlight: application for the treatment of industrial wastewater. J Photochem Photobiol A: Chem 154(2–3):219–228

Aliabadi M, Sagharigar T (2011) Photocatalytic removal of Rhodamine B from aqueous solutions using TiO_2 nanocatalyst. J Appl Environ Biol Sci 1(12):620–626

Attarchi N, Montazer M, Toliyat T (2013) Ag/TiO_2/β-CD nano composite: preparation and photo catalytic properties for methylene blue degradation. Appl Catal A: Gen 467:107–116

Beltran-Heredia J, Sanchez-Martin J, Rodriguez-Sanchez MT (2011) Textile wastewater purification through natural coagulants. Appl Water Sci 1(1–2):25–33

Chen Y, Wang K, Lou L (2004) Photodegradation of dye pollutants on silica gel supported TiO_2 particles under visible light irradiation. J Photochem Photobiol A: Chem 163(1–2):281–287

Damardji B, Khalaf H, Duclaux L, David B (2009) Preparation of TiO_2-pillared montmorillonite as photocatalyst part II—photocatalytic degradation of a textile azo dye. Appl Clay Sci 45(1–2):98–104

Daneshvar N, Salari D, Khataee AR (2003a) Photocatalytic degradation of azo dye acid red 14 in water: investigation of the effect of operational parameters. J Photochem Photobiol A: Chem 157(1):111–116

Daneshvar N, Salari D, Khataee AR (2003b) Photocatalytic degradation of azo dye acid red 14 in water: investigation of the effect of operational parameters. J Photochem Photobiol A: Chem 157(1):111–116

Dlamini LN, Krause RW, Kulkarni GU, Durbach SH (2011) Photodegradation of bromophenol blue with fluorinated TiO_2 composite. Appl Water Sci 1(1–2):19–24

Dong B, Li Z, Li Z, Xu X, Song M, Zheng W, Wang C, Al-Deyab SS, El-Newehy M (2010) Highly efficient $LaCoO_3$ nanofibers catalysts for photocatalytic degradation of Rhodamine B. J Am Cer Soc 93(11):3587–3590

Dukkanci M, Gunduz G, Yilmaz S, Prihodko RV (2010) Heterogeneous fenton-like degradation of Rhodamine 6G in water using CuFeZSM-5 zeolite catalyst prepared by hydrothermal synthesis. J Hazard Mater 181(1–3):343–350

Grzechulska J, Morawski AW (2002) Photocatalytic decomposition of azo-dye acid black 1 in water over modified titanium dioxide. Appl Catal B: Environ 36(1):45–51

He Z, Sun C, Yang S, Ding Y, He H, Wang Z (2009) Photocatalytic degradation of Rhodamine B by Bi_2WO_6 with electron accepting agent under microwave irradiation: mechanism and pathway. J Hazard Mater 162(2–3):1477–1486

Hoffmann MR, Martin ST, Choi W, Bahnemann DW (1995) Environmental applications of semiconductor photocatalysis. Chem Rev 95(1):69–96

Jain R, Mathur M, Sikarwar S, Mittal A (2007) Removal of the hazardous dye Rhodamine B through photocatalytic and adsorption treatments. J Environ Manag 85(4):956–964

Kansal SK, Singh M, Sud D (2007) Studies on photodegradation of two commercial dyes in aqueous phase using different photocatalysts. J Hazard Mater 141(3):581–590

Kansal SK, Singh M, Sud D (2008) Studies on TiO_2/ZnO photocatalyzed degradation of lignin. J Hazard Mater 153(1–2):412–417

Karunakaran C, Gomathisankar P, Manikandan G (2010) Preparation and characterization of antimicrobial Ce-doped ZnO nanoparticles for photocatalytic detoxification of Cyanide. Mater Chem Phys 123(2–3):585–594

Kelesoglu S, Kes M, Sutcu L, Polat H (2012) Adsorption of methylene blue from aqueous solution on high lime fly ash: kinetic, equilibrium, and thermodynamic studies. J Disper Sci Technol 33(1):15–23

Kou T, Jin C, Zhang C, Sun J, Zhang Z (2012) Nanoporous core–shell Cu@Cu_2O nanocomposites with superior photocatalytic properties towards the degradation of methyl orange. RSC Adv 2(33):12636–12643

Li J, Ma W, Lei P, Zhao J (2007) Detection of intermediates in the TiO_2-assisted photodegradation of Rhodamine B under visible light irradiation. J Environ Sci 19(7):892–896

Lu P, Wu F, Deng N (2004) Enhancement of TiO_2 photocatalytic redox ability by β-cyclodextrin in suspended solutions. Appl Catal B: Environ 53(2):87–93

Luan J, Li M, Ma K, Li Y, Zou Z (2011) Photocatalytic activity of novel Y_2InSbO_7 and Y_2GdSbO_7 nanocatalysts for degradation of environmental pollutant Rhodamine B under visible light irradiation. Chem Eng J 167(1):162–171

Macwan DP, Dave PN, Chaturvedi S (2011) A review on nano-TiO_2 sol–gel type syntheses and its applications. J Mater Sci 46(11):3669–3686

Mehrdad A, Massoumi B, Hashemzadeh R (2011) Kinetic study of degradation of Rhodamine B in the presence of hydrogen peroxide and some metal oxide. Chem Eng J 168(3):1073–1078

Pitchaimuthu S, Rajalakshmi S, Kannan N, Velusamy P (2013) Enhanced photocatalytic activity of titanium dioxide by β-Cyclodextrin in decoloration of Acid Yellow 99 dye. Desalin Water Treat 52(16–18):3392–3402

Pitchumani K, Velusamy P, Srinivasan C (1994) Selectivity in sodium borohydride reduction of coumarin encapsulated in β-cyclodextrin. Tetrahedron 50(45):12979–12988

Rajalakshmi S, Pitchaimuthu S, Kannan N, Velusamy P (2013) Photocatalytic effect of β-cyclodextrin on semiconductors for the removal of Acid Violet dye under UV light irradiation. Desalin Water Treat 52(16–18):3432–3444

Rauf MA, Salman Ashraf S (2009) Fundamental principles and application of heterogeneous photocatalytic degradation of dyes in solution. Chem Eng J 151(1–3):10–18

Salomatova VA, Pozdnyakova IP, Yansholeb VV, Wu F, Grivin VP, Bazhin NM, Plyusnin VF (2014) Photodegradation of 4,4-bis(4-hydroxyphenyl)valeric acid and its inclusion complex with β-cyclodextrin in aqueous solution. J Photochem Photobiol A: Chem 274:27–32

Santhi T, Prasad AL, Manonmani S (2011) A comparative study of microwave and chemically treated *Acacia nilotica* leaf as an eco friendly adsorbent for the removal of Rhodamine B dye from aqueous solution. Arab J Chem. doi:10.1016/j.arabjc.2010.11.008

Serra-Gomez R, Tardajos G, Gonzalez-Benito J, Gonzalez-Gaitano G (2012) Rhodamine solid complexes as fluorescence probes to monitor the dispersion of cyclodextrins in polymeric nanocomposites. Dyes Pigm 94(3):427–436

Silva NU, Nunes TG, Saraiva MS, Shalamzari MS, Vaza PD, Monteiro OC, Nunes CD (2011) Photocatalytic degradation of rhodamine B using Mo heterogeneous catalysts under aerobic conditions. Appl Catal B: Environ 113–114:180–191

Sun M, Li D, Chen Y, Chen W, Li W, He Y, Fu X (2009) Synthesis and photocatalytic activity of calcium antimony oxide hydroxide for the degradation of dyes in water. J Phys Chem C 113(31):13825–13831

Velmurugan R, Swaminathan M (2011) An efficient nano structured ZnO for dye sensitized degradation of Reactive Red 120 dye under solar light. Sol Energy Mater Sol Cell 95(3):942–950

Velusamy P (1998) Study of thermal and photochemical reactions in cyclodextrin. Ph.D. thesis submitted to Madurai Kamaraj University, Madurai, p 50

Velusamy P, Pitchumani K, Srinivasan C (1996) Selectivity in bromination of aniline and N-substituted anilines encapsulated in β-cyclodextrin. Tetrahedron 52(10):3487–3496

Velusamy P, Rajalakshmi S, Pitchaimuthu S, Kannan N (2011) Photo decoloration of organic dyes on β-cyclodextrin modified ZnO. Indian J Environ Prot 31(10):801–809

Velusamy P, Rajalakshmi S, Pitchaimuthu S, Kannan N (2013) Photo decoloration of Brilliant Green dye using β-CD modified TiO_2. Indian J Environ Protect 33(7):583–589

Velusamy P, Pitchaimuthu S, Rajalakshmi S, Kannan N (2014) Modification of the photocatalytic activity of TiO_2 by β-cyclodextrin in decoloration of Ethyl Violet dye. J Adv Res 5(1):19–25

Wang G, Wu F, Zhang X, Luo M, Deng N (2006a) Enhanced TiO_2 photocatalytic degradation of bisphenol E by β-cyclodextrin in suspended solutions. J Hazard Mater B 133(1–3):85–91

Wang G, Wu F, Zhang X, Luo M, Deng N (2006b) Enhanced TiO_2 photocatalytic degradation of bisphenol A by β-cyclodextrin in suspended solutions. J Photochem Photobiol A: Chem 179(1–2):49–56

Wang H, Niu J, Long X, He Y (2008) Sonophotocatalytic degradation of Methyl Orange by nano-sized Ag/TiO_2 particles in aqueous solutions. Ultrason Sonochem 15(4):386–392

Wang J, Li J, Zhang L, Li C, Xie Y, Liu B, Xu R, Zhang X (2009a) Photocatalytic degradation of organic dyes by a high efficient TiO_2-based catalysts under solar light irradiation. Catal Lett 130(3–4):551–557

Wang X, Wang J, Guo P, Guo W, Wang C (2009b) Degradation of Rhodamine B in aqueous solution by using swirling jet-induced

cavitation combined with H_2O_2. J Hazard Mater 169(1–3):486–491

Xin F, Zhang H, An W, Sun L, Hao A, Li Y (2012) Vesicles prepared from inclusion complexes between cyclodextrins and ethyl benzoate. J Disper Sci Technol 33(1):1–4

Yang Z, Zhang X, Cui J (2014) Self-assembly of bioinspired catecholic cyclodextrin TiO_2 heterosupramolecule with high adsorption capacity and efficient visible-light photoactivity. Appl Catal B: Environ 148–149:243–249

Yu K, Yang S, He H, Sun C, Gu C, Ju Y (2009) Visible light-driven photocatalytic degradation of Rhodamine B over $NaBiO_3$: pathways and mechanism. J Phys Chem A 113(37):10024–10032

Zhang X, Wu F, Wang B, Deng N, Luo M (2007) Research of inclusion complexation of 4, 4′-thiodiphenol effected by β-cyclodextrin in aqueous solutions and the effect on photodegradation. Wuhan Univ J Nat Sci 12(3):535–540

Zhang X, Wu F, Wang Z, Guo Y, Deng N (2009) Photocatalytic degradation of 4, 4-biphenol in TiO_2 suspension in the presence of cyclodextrins: a trinity integrated mechanism. J Mol Catal A: Chem 301(1–2):134–139

Zhang X, Wu F, Deng N (2011) Efficient photodegradation of dyes using light-induced self-assembly TiO_2/β-cyclodextrin hybrid nanoparticles under visible light irradiation. J Hazard Mater 185(1):117–123